FABRICATION OF IMPROVED QUADRANT-TYPE X-BAND HIGH-GRADIENT ACCELERATING STRUCTURES

Tetsuo Abe*, Toshikazu Takatomi, Yasuo Higashi, Toshiyasu Higo, and Shuji Matsumoto
High Energy Accelerator Research Organization (KEK), Tsukuba, Japan

Abstract

A common normal-conducting high-gradient accelerating structure of particle accelerators is the "disk type", which has dozens of machined, stacked, and bonded disks. In the disk type, surface currents associated with a magnetic field of an accelerating mode flow across disk-to-disk junctions. Another structure is the "quadrant type", which is *orthogonal* to the above type. In the quadrant type, bonding planes are parallel to a beam axis, and therefore, this type has the remarkable feature that no such surface current flows across any junction. We proposed, designed, fabricated, and tested an *improved* quadrant-type X-band (11.4 GHz) single-cell standing-wave structure, and then demonstrated its efficacy and the potential for this structure to be successful for accelerating gradients of 100 MV/m or higher at sufficiently low breakdown rates. For a complete demonstration, we have fabricated a 24-cell traveling-wave structure based on the improved-quadrant-type fabrication method.

INTRODUCTION

High-gradient accelerating structures with accelerating gradients (E_{acc}) of 100 MV/m or higher are indispensable for future high-energy accelerators to search for new physics in particle physics, and are also useful to make compact accelerators of medical linacs and XFELs, etc. Most of these structures, made of oxygen free copper, are fabricated by machining and stacking dozens of disks, and then bonding them by diffusion bonding or brazing ("disk-type" structures). An example of the disk-type structure is shown in Fig. 1a. Disk-type accelerating structures have the potential problem that surface currents associated with a magnetic field of an accelerating mode flow across disk-to-disk junctions, where perfect bonding of neighboring disks at the inner surface is not guaranteed by any bonding method. For example, one report [1] observed small gaps between the diffusion-bonded disks together with some microscopic objects in the SEM images. Although we do not know the details of the radio-frequency (RF) breakdown mechanism that is a dominant contributor to the breakdown rates of accelerating structures, such defects are a serious concern because huge surface currents of $\approx 10^8$ A/cm^2 or higher during high-gradient operations flow across disk-to-disk junctions. Furthermore, a significant impact of the surface magnetic field, or surface current, on breakdown rates has been discovered [2, 3].

Another structure type is the "quadrant type" ("half type" in the case of undamped structures), which is *orthogonal* to the disk type. For quadrant-type structures, no surface current associated with a magnetic field flows across any junction except for perturbative effects. In addition, we can expect significant cost reduction in quadrant-type structure fabrication with simpler machining and bonding compared to disk-type structures. Furthermore, this structure is easy to fabricate from hard materials (e. g., CuAg) without a high-temperature process by using only electron-beam welding (EBW) to maintain its material hardness. This fabrication process is important because it has been found that we can achieve lower breakdown rates for structures with higher yield strength [4].

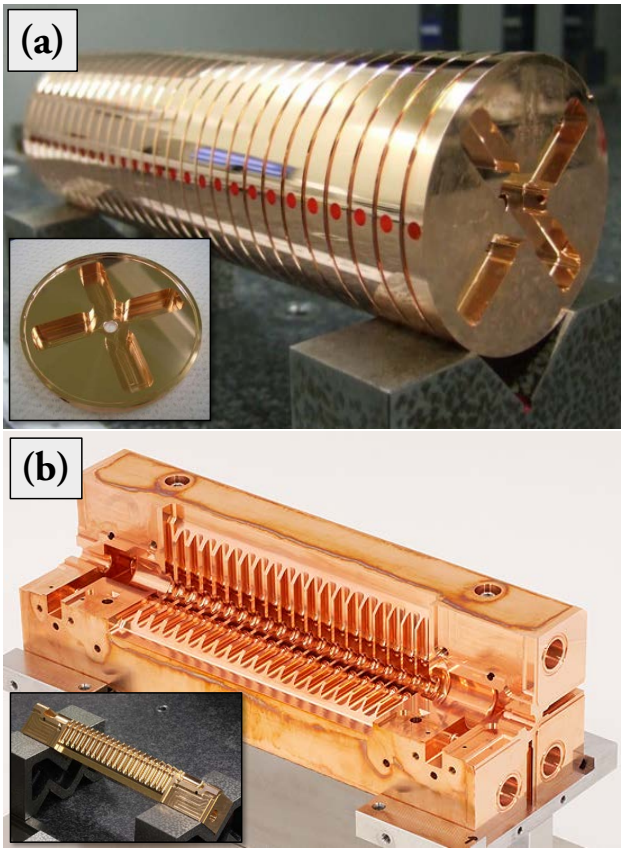

Figure 1: Two types of orthogonal high-gradient accelerating structures: (a) disk type and (b) quadrant type.

In 2008, we fabricated a quadrant-type X-band accelerating structure, made of CuZr, with a higher-order-mode (HOM) damped structure by waveguides (waveguide damped structure) consisting of 18 cells (Fig. 1b) [5]. In 2009, we performed a high-gradient test of the structure at KEK/Nextef/Shield-A. As a result, however, E_{acc} was limited to 60 MV/m or lower with a 50 ns rectangular pulse, and we observed no conditioning effects [6]. SLAC also performed the same type of high-gradient test, and obtained

* tetsuo.abe@kek.jp

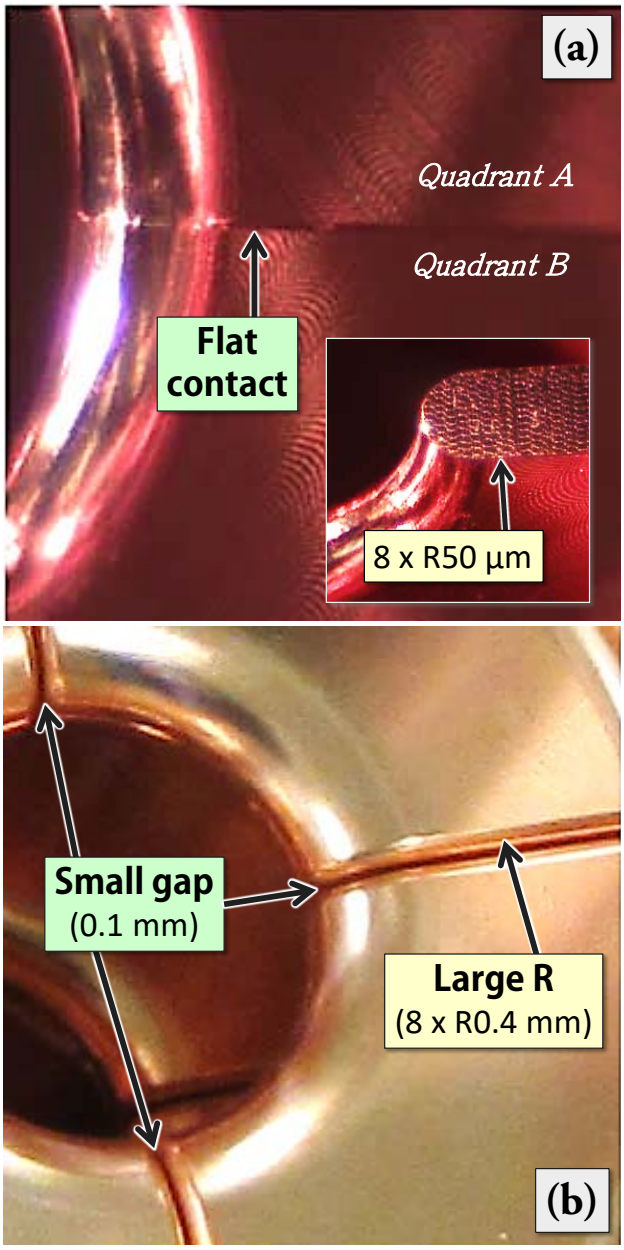

Figure 2: Photographs around the iris of the (a) naive and (b) improved quadrant-type structures.

the same result even with electropolishing of the structure. Usually, we reach E_{acc} = 100 MV/m in RF conditioning of X-band accelerating structures even with a waveguide damped structure. Therefore, such a quadrant-type structure has some fatal flaws.

Although we could not find any evidence, including the material properties of CuZr, for the fatal flaws experimentally, we proposed an *improved*-quadrant-type structure [7,8] based on simulation studies [9] to overcome all disadvantages of the *naive* quadrant-type design. The naive and improved designs are shown in Fig. 2, and the improved one has the following two key characteristics:

- A large round chamfer of 0.4 mm at the corner of quadrants is added to suppress field enhancements down to +25% for any actual case, where +20% enhancement is a theoretical minimum for any quadrant-type structure with round chamfer, and
- A small finite gap of 0.1 mm between neighboring quadrants is added to avoid any virtual leak.

The chamfer of 0.4 mm and the gap of 0.1 mm are the results of optimization by simultaneously minimizing the field enhancements (< +25%) and deterioration of the shunt impedance (< 0.2%). To demonstrate the performance, we fabricated an X-band accelerating structure based on the improved design in the form of a single-cell standing-wave test cavity [10]. This structure consists of three cells, which are coupling, test, and end cells, where the resonant frequencies of the coupling and end cells are slightly detuned so that the strength of the excited field in the test cell is approximately twice those in the coupling and end cells. The coupling and end cells are necessary to make the excited field in the test cell similar to those in a corresponding multi-cell accelerating structure. In other words, this type of single-cell structure with three cells is a minimal structure keeping a realistic RF field for acceleration. It should be noted that single-cell structures are much easier to fabricate and test than multi-cell structures, and therefore, are suitable for basic studies by high-gradient testing.

In 2017, we performed a high-gradient test of the above-mentioned single-cell structure at KEK/Nextef/Shield-B [11]. During the RF conditioning, E_{acc} smoothly reached 125 MV/m. This value of E_{acc} is much higher than the highest gradient of 60 MV/m in the high-gradient test of the 18-cell naive-quadrant-type X-band traveling-wave accelerating structure for the 50 ns rectangular pulse. We observed a further conditioning effect even at $E_{\mathrm{acc}} \approx 125$ MV/m, and no performance limit. Therefore, we demonstrated the possibility of succeeding with the improved-quadrant-type fabrication method. From the breakdown-rate measurement performed after the RF conditioning, we can expect sufficient high-gradient performance of the improved quadrant type of accelerating structure to meet the CLIC specification (3×10^{-7} breakdowns/pulse/m or lower) at E_{acc} = 100 MV/m, taking our study to the next level for a complete demonstration of its principle and efficacy with a multi-cell traveling structure.

In this paper, we present results of fabrication of an improved-quadrant-type X-band (11.4 GHz) 24-cell traveling-wave structure. The design of the structure is based on a CLIC prototype structure TD24R05 [12], which has a waveguide damped structure and is close to the final design for CLIC [13]. It should be noted that a waveguide damped structure is promising for HOM damping in a high-beam current and/or multi-bunch acceleration such as that in linear colliders.

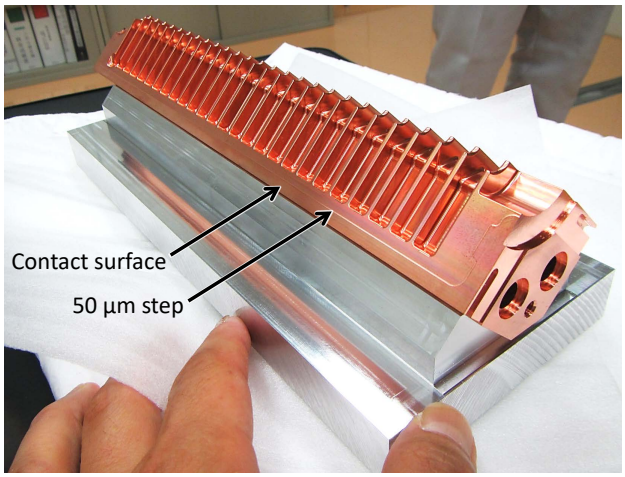

Figure 3: A quadrant fabricated with ultraprecision milling.

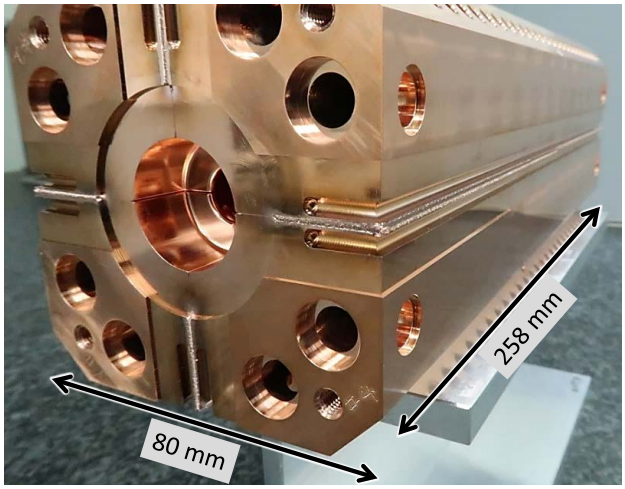

Figure 4: Photograph of the quadrants after the EBW.

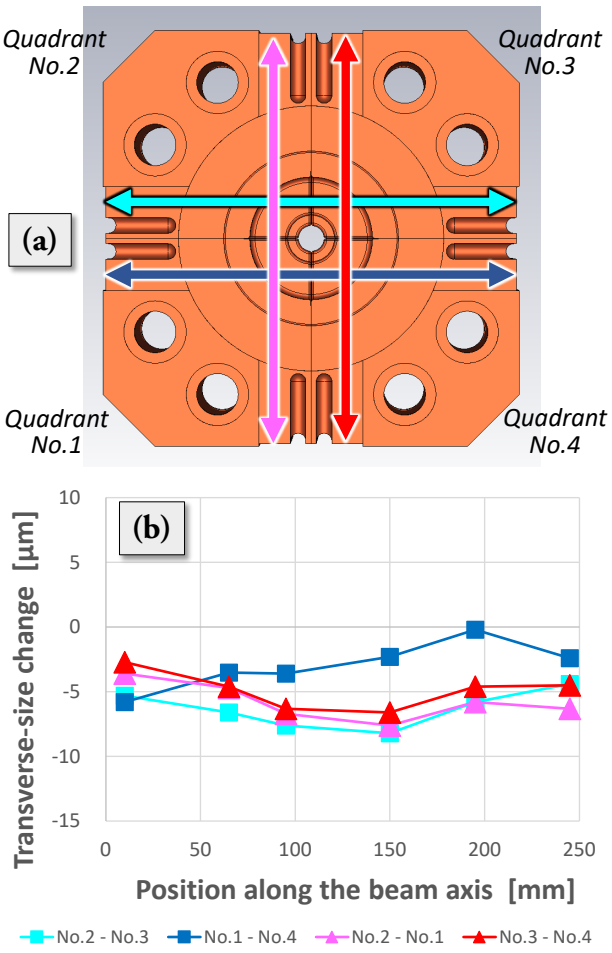

Figure 5: Transverse-size change measured with a CMM. (a) Definition of the measured sizes shown with arrows. (b) Results of the measurement (after minus before), where the color of the plots corresponds to the same color of the arrows in (a).

ELECTRICAL DESIGN

In addition to TD24R05, the electrical design is based on CLIC-G∗ [14], where the most remarkable feature is the cell-wall profile described with a fourth order polynomial function (see Fig. 6 in [14] for details) so as to make the surface magnetic field more uniform (i. e. to make the peak magnetic field strength lower). The phase advance per cell is 120°.

ULTRAPRECISION MILLING

Quadrants were fabricated with ultraprecision milling performed by U-CORPORATION Co., Ltd. [15], where it took approximately two weeks to complete one quadrant. Figure 3 is a photograph of a fabricated quadrant. We achieved maximum peak roughness (R_y) and profile accuracy of R_y ≈ 1 µm and ≈ 5 µm, respectively.

BONDING OF THE QUADRANTS

Four quadrants were bonded with EBW performed by TAIYO EB teck Co., Ltd. [16], where it took only several hours to complete the EBW. During the EBW, the cathode voltage (beam current) of the EBW machine was 150 kV (10 mA), the table speed was 12.5 mm/s, and the focus point of the electron beam was approximately 20 mm away from the irradiated surface. Figure 4 is a photograph of the bonded quadrants after the EBW. We measured the temperature of the quadrants during the EBW, and found the maximum temperature rise was 25 °C.

We measured the size of the structure before and after the EBW by using a coordinate measuring machine (CMM). The amount of changes in the size along the beam axis was shorter than 2 µm, while that in the transverse size was 5 µm shrinkage in average as shown in Fig. 5. It should be noted that the variation in the transverse size change is mostly within a few micrometers; however, the amount of the size change shown with dark blue plots shows significantly different pattern, which presumably originates from the order of the EBW, and is to be investigated.

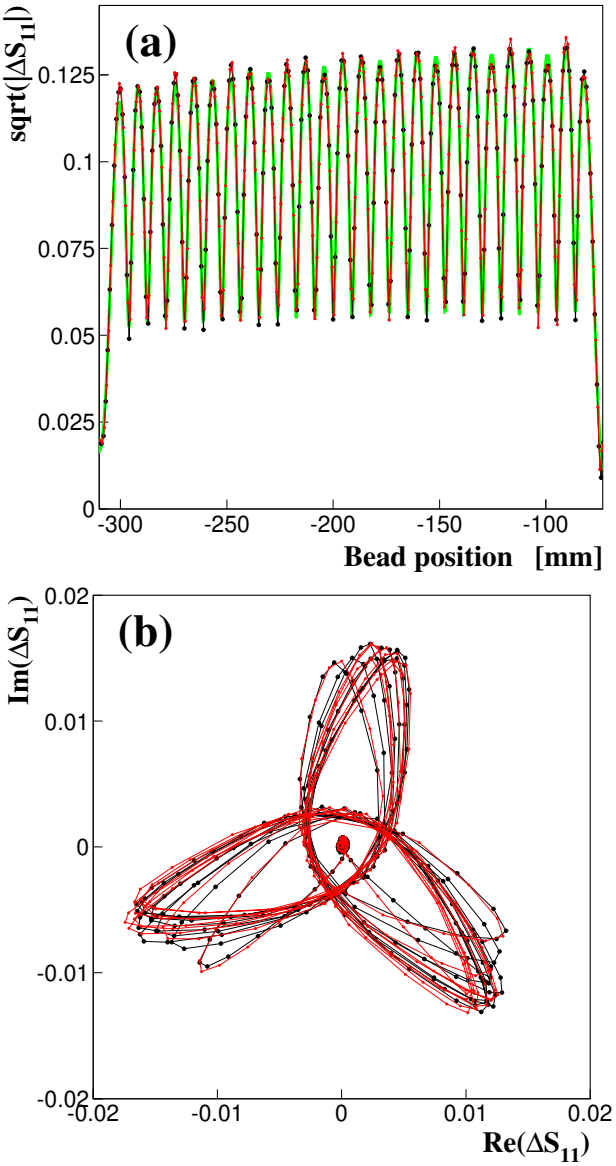

Figure 6: Results of the bead pull measurement before (black) and after (red) the EBW, where frequency tuning was not yet performed. ΔS_{11} indicates change of the reflection coefficient when the bead enters each cell. (a) Field distribution along the beam axis, where the green line indicates the design normalized to the measurement. (b) Phase advance at 11.4061 GHz (11.4112 GHz) before (after) the EBW.

RF MEASUREMENTS

We measured the RF characteristics by using a vector network analyzer. Figure 6a and b show measured field distribution and phase advance, respectively, before and after the EBW, both of which are reasonable. It should be noted that the measured results in Fig. 6 after the EBW are good agreement with those before the EBW, which means that the structure did not deform significantly during the EBW. The frequency at a phase advance close to 120° increased by 5.1 MHz, which is much lower than the range of frequency tuning (±40 MHz).

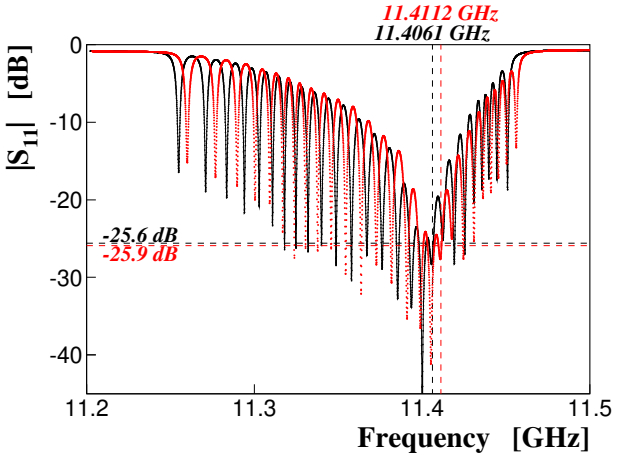

Figure 7: Measured reflection coefficient before (black) and after (red) the EBW, where frequency tuning was not yet performed. The vertical dashed lines indicate frequencies with a phase advance close to 120°, and the horizontal dashed lines indicate return losses at the frequencies with a phase advance close to 120° before (black) and after (red) the EBW. Frequencies in the raw data were converted to those for the structure with a temperature of 30°C and vacuum inside, and shown in the horizontal axis.

Figure 7 shows measured reflection coefficient S_{11} in dB, the input matching, before and after the EBW. The return loss at a phase advance close to 120° is smaller than −25 dB although frequency tuning was not yet performed.

SUMMARY

Since we demonstrated the enough high-gradient performance with the improved-quadrant-type fabrication method using the single-cell standing-wave test cavity, we fabricated the 24-cell traveling-wave structure for a complete demonstration of its principle and efficacy. The measured RF characteristics were found to be reasonable even after bonding of the four quadrants with EBW, and the frequency increase by the EBW was 5.1 MHz in average, which is much lower than the range of frequency tuning. Comparing the results of the RF measurements before and after the EBW, it is concluded that the EBW had no significant effect on the RF characteristics.

The high-gradient test is to be planned.

ACKNOWLEDGEMENTS

We greatly appreciate the financial and technical support from the CLIC team. This is endorsed by the agreement on collaborative work between CERN and KEK (ICA-JP-0103).

REFERENCES

[1] M. Aicherer, "TD18 Post-Mortem SEM Observation: Update," tech. rep., CERN, November 2010. CERN EDMS.

[2] V. Dolgashev *et al.*, "Geometric Dependence of Radio-Frequency Breakdown in Normal Conducting Accelerating Structures," *Appl. Phys. Lett.*, vol. 97, p. 171501, 2010.

[3] F. Wang *et al.*, "Performance limiting effects in X-band accelerators," *Phys. Rev. ST Accel. Beams*, vol. 14, p. 010401, 2011.

[4] V. A. Dolgashev, "High Gradient, X-Band and Above, Metallic RF Structures," in *the 2nd European Advanced Accelerator Concepts Workshop, Italy*, 2015.

[5] T. Higo *et al.*, "Fabrication of a Quadrant-type Accelerator Structure for CLIC," *Conf. Proc.*, vol. C0806233, 2008.

[6] T. Higo, "KEK activities on CLIC X-band Accelerating Structures." CERN Indico, March 2010. Presented in Mini-Workshop on CLIC X-band Structure R&D at THU.

[7] T. Abe *et al.*, "Quadrant-Type X-Band Single-Cell Structure for High Gradient Tests," in *Proceedings of the 9th Annual Meeting of Particle Accelerator Society of Japan*, 2012. THPS095 (Japanese).

[8] T. Abe *et al.*, "Fabrication of Quadrant-Type X-Band Single-Cell Structure used for High Gradient Tests," in *Proceedings of the 11th Annual Meeting of Particle Accelerator Society of Japan*, 2014. SUP042.

[9] T. Abe, "Study of Surface Field Enhancements due to Fine Structures," in *Proceedings of the 8th Annual Meeting of Particle Accelerator Society of Japan*, 2011. TUPS086.

[10] V. A. Dolgashev *et al.*, "Travelling wave and standing wave single cell high gradient tests," in *Linac 2004*.

[11] T. Abe *et al.*, "High-Gradient Test Results on a Quadrant-Type X-Band Single-Cell Structure," in *Proceedings of the 14th Annual Meeting of Particle Accelerator Society of Japan*, 2017. WEP039.

[12] T. Higo *et al.*, "Comparison of High Gradient Performance in Varying Cavity Geometries," in *IPAC 2013*. WEPFI018.

[13] M. Aicheler *et al.*, "A Multi-TeV Linear Collider Based on CLIC Technology : CLIC Conceptual Design Report," *CERN-2012-007*, 2012.

[14] H. Zha and A. Grudiev, "Design and optimization of Compact Linear Collider main linac accelerating structure," *Phys. Rev. Accel. Beams*, vol. 19, no. 11, p. 111003, 2016.

[15] `http://www.u-corp.co.jp/TEC/en/` .

[16] `http://taiyo-eb.co.jp/` .